ELSEVIER

Journal of Photochemistry and Photobiology A: Chemistry 94 (1996) 101–105

Journal of PHOTOCHEMISTRY AND PHOTOBIOLOGY A:CHEMISTRY

Measurement of the cage effect in the photolysis of the $(\eta^5\text{-}C_5H_4(CH_2)_2N(H)C(O)(CH_2)_3CH_3)_2Mo_2(CO)_6$ complex

Britt E. Lindfors [a], Gregory F. Nieckarz [a], David R. Tyler [a,*], Anne G. Glenn [b]

[a] *Department of Chemistry, University of Oregon, Eugene, OR 97403, USA*

[b] *Department of Chemistry, Guilford College, Greensboro, NC 27410, USA*

Received 31 July 1995; accepted 11 September 1995

Abstract

A previously reported method for determining radical pair cage efficiency factors F_c in hexane has been extended to tetrahydrofuran (THF). The technique involves measuring quantum yields as a function of viscosity, and it is necessary therefore to find viscosity enhancers that do not selectively solvate a cage pair. For radical cage pairs generated by photolysis of $Cp_2Mo_2(CO)_6$-type complexes, it is shown that tetraglyme is a suitable viscosity enhancer in THF. The THF–tetraglyme solvent system is a useful system for cage pair precursors that require a more polar solvent than hexane for solubility. A device is also described that will measure quantum yields automatically in the range 400–1100 nm. The heart of the apparatus is a radiometer that collects transmitted light intensity as a function of time and stores the data in a personal computer.

Keywords: Cage effect; Photolysis; Tetrahydrofuran

1. Introduction

Radical cage effects have an enormous impact on chemical reactivity in solution, and in fact they are necessary to explain many fundamental reaction phenomena. These phenomena include rate–viscosity correlations [1], variations in products and product yields as a function of medium [2], variations in quantum yields as a function of medium [3,4], various peculiarities in racemization and scrambling reactions as a function of medium [5], and magnetic isotope [6] and CIDNP [7] effects. In addition, three of the most important, but least recognized, consequences of the cage effect are that quantitative knowledge of the cage effect is needed (1) to calculate $\Delta H^{\ddagger}$ and $\Delta S^{\ddagger}$ values properly from $\Delta H_{obs}{}^{\ddagger}$ and $\Delta S_{obs}{}^{\ddagger}$ [8–10], (2) to extract elementary step rate constants from k_{obs} and (3) to calculate correct bond dissociation energies from kinetics data [8].

Quantitative information about the radical cage is usually presented in the form of the "cage efficiency factor", denoted F_c [11]. F_c is defined as the ratio of the efficiency of radical cage pair combination to that of all competing cage processes. For example, in Scheme 1, F_c is given by the ratio $k_c/(k_c+k_d)$ [12].

$$\mathrm{R\text{–}R} \underset{k_c}{\overset{k_1 \text{ or } h\nu}{\rightleftharpoons}} \underset{\text{cage pair}}{(\mathrm{R}\cdot\cdot\mathrm{R})} \underset{k_{-1}}{\overset{k_d}{\rightleftharpoons}} \underset{\text{free radicals}}{2\mathrm{R}^{\cdot}} \longrightarrow \text{Products}$$

Scheme 1.

We recently reported a new method for measuring F_c in systems wherein a radical cage pair is generated by photolysis of a bond [13]. The example that we reported involved the $[Cp(CO)_3M\cdot\cdot M(CO)_3Cp]$ radical cage pair generated by photolysis of the metal–metal bond in $Cp_2M_2(CO)_6$ ($M=Mo, W$; $Cp=\eta^5\text{-}C_5H_5$).

As discussed in the previous paper [13], our new procedure for obtaining F_c is to measure quantum yields for the reaction with a radical trap as a function of solvent system viscosity (at constant temperature). By appropriate analysis of these data, it is possible to extract F_c values for the system. The solvent used in our previous study was *n*-hexane, with Nujol (heavy mineral oil) added to increase the viscosity. (Nujol was used to increase the viscosity because it is a straight-chain hydrocarbon, as is *n*-hexane. Thus we sought to avoid "selective solvation".) Not all complexes are hexane–Nujol soluble, and for that reason we investigated other solvent systems in which the viscosity can be varied without selective solvation. In this paper, we report cage effect measurements using the tetrahydrofuran (THF)–tetraglyme solvent system. In the experimental section, we also report a

* Corresponding author.

SSDI 1010-6030(95)04213-X

new and convenient apparatus for automatically measuring quantum yields [14].

2. Results and discussion

Cage effects are important in determining the degradation efficiency of polyamides that have metal–metal bonds along the polymer backbone [16]. In order to study quantitatively the effect of chain length on the cage effect, we needed cage effect data for **1**, a model complex for the polymers that we are studying. This molecule is insoluble in hexane–Nujol solvent mixtures, and therefore our previously described method using this solvent system was inapplicable.

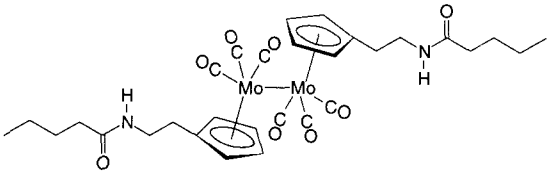

1

Tetraglyme, a polyether ($CH_3(OCH_2CH_2)_4OCH_3$), has sufficient viscosity and polarity that it could be used as an alternative solvent for increasing viscosity in mixtures with THF. Complex **1** is readily soluble in THF–tetraglyme mixtures of varying proportions, and the similarity of the two solvents suggested that selective solvation should not be a problem. Irradiation ($\lambda = 540$ nm) of **1** in the presence of CCl_4 in THF–tetraglyme mixtures of varying concentration proceeded as follows:

$$Cp_2'Mo_2(CO)_6 + 2CCl_4 \xrightarrow[\lambda = 540\ nm]{h\nu} 2Cp'Mo(CO)_3Cl + 2[\cdot CCl_3] \quad (1)$$

$$Cp' = (\eta^5\text{-}C_5H_4(CH_2)_2N(H)C(O)(CH_2)_3CH_3)$$

The reaction was monitored by IR spectroscopy, which showed the disappearance of the dimer bands at 2009, 1967, 1953 and 1901 cm^{-1} and the appearance of new bands at 2049 and 1972 cm^{-1}. The product bands are assigned to $(CpCH_2CH_2NHC(O)(CH_2)_4CH_3)Mo(CO)_3Cl$ by comparison with those of the analogous $CpMo(CO)_3Cl$ ($\nu(C{\equiv}O) = 2055$ and 1983 cm^{-1} in CCl_4 [17]).

The photochemical reaction of $Cp_2Mo_2(CO)_6$ with CCl_4 to form $CpMo(CO)_3Cl$ has been extensively studied, and the pathway is shown in Scheme 2 [18]. The same pathway, involving photolysis of the Mo–Mo bond followed by chlorine atom abstraction, is logically proposed for reaction (1).

$$Cp_2Mo_2(CO)_6 \overset{h\nu}{\rightleftharpoons} 2CpM\dot{o}(CO)_3$$

$$CpM\dot{o}(CO)_3 + CCl_4 \longrightarrow CpMo(CO)_3Cl + \cdot CCl_3$$

Scheme 2. Mechanism of the photochemical reaction of $Cp_2Mo_2(CO)_6$ with CCl_4.

With sufficiently high concentrations of CCl_4, collisional cage pair formation (k_{-1}) can be suppressed so that all radicals that escape the cage will form the trapped product. Under conditions of complete free radical trapping, the following equation can be derived, where Φ_{obs} is the observed quantum yield for disappearance of the dimer and Φ_{pair} is the quantum yield for the formation of the caged radical pair:

$$\frac{1}{\Phi_{obs}} = \frac{1}{\Phi_{pair}}\left(1 + \frac{k_c}{k_d}\right) \quad (2)$$

The ratio k_c/k_d (and thus F_c, which is equal to $[1 + (k_d/k_c)]^{-1}$) is obtained by substituting the values of Φ_{obs} and Φ_{pair} into Eq. (2). As discussed previously [13], the value of Φ_{pair} is obtained by extrapolating the plot of Φ_{obs}^{-1} vs. viscosity to zero viscosity.

Quantum yields for reaction (1) as a function of viscosity are shown in Table 1 and plotted as a function of viscosity in Fig. 1. The reciprocal plot is shown in Fig. 2, the intercept of which yields $\Phi_{pair} = 0.78 \pm 0.04$. (Note that the linearity of the plot in Fig. 2 strongly suggests that selective solvation does not occur.) Using this value of Φ_{pair}, F_c values were obtained using Eq. (2). A plot of F_c vs. viscosity is shown in Fig. 3. As expected, the cage effect increases with an increase in viscosity.

Table 1
Quantum yields ($\lambda = 540$ nm) and F_c values (23 °C) at various viscosities for the reaction of **1** with CCl_4 in THF–tetraglyme mixtures [a]

Solvent (% tetraglyme)	Viscosity (cP)	Φ_{obs}	F_c
0	0.428	0.73 ± 0.02	0.070
50	1.44	0.57 ± 0.06	0.265
60	1.67	0.51 ± 0.03	0.343
70	2.22	0.47 ± 0.05	0.393
80	3.51	0.41 ± 0.02	0.476

[a] Error limits represent 2σ.

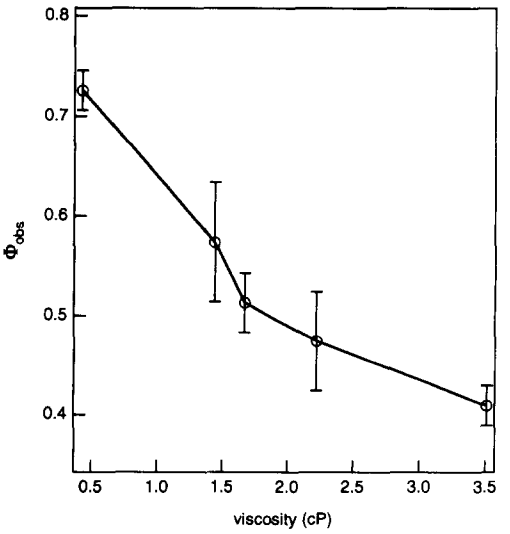

Fig. 1. Plot of Φ vs. viscosity for the photochemical reaction ($\lambda = 540$) of **1** with CCl_4 (2 M). All error bars represent $\pm 2\sigma$.

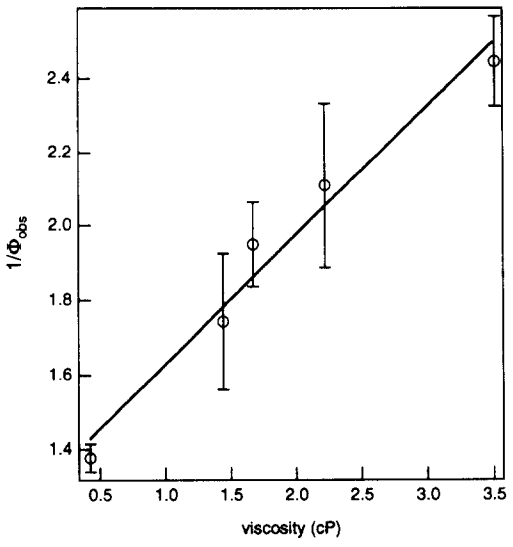

Fig. 2. Plot of Φ^{-1} vs. viscosity for the photochemical reaction ($\lambda = 540$) of **1** with CCl_4 (2 M). All error bars represent $\pm 2\sigma$.

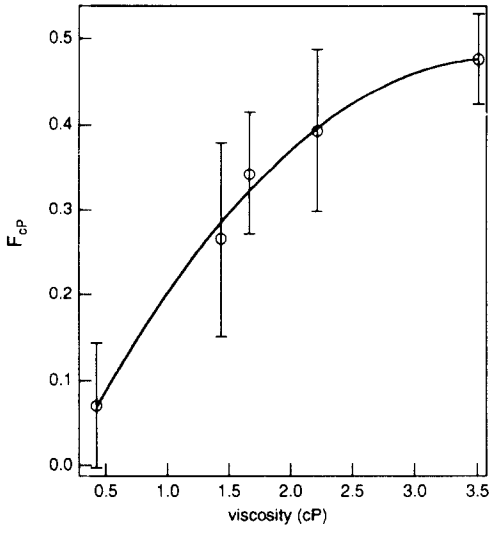

Fig. 3. Plot of F_c as a function of viscosity for **1** at 23 °C.

In summary, the THF–tetraglyme solvent system is a solvent system than can be used when it is necessary to use a more polar solvent system than hexane–Nujol. One final point concerns the measurement of F_c. A major problem with the procedure for obtaining F_c is that it is extremely labor intensive; to obtain F_c values for one radical cage pair typically requires the measurement of 20 quantum yields. To circumvent this problem, we built a computer-controlled device to measure quantum yields automatically. The apparatus quickly and easily measures quantum yields in the range 400–1100 nm, and it can be used for virtually all types of reaction. The details of the device are reported as part of Section 3 [14].

3. Experimental section

3.1. General comments

All manipulations were carried out in the absence of water and oxygen using standard Schlenk and dry-box techniques. Complex **1** was prepared using a method reported previously [19]. Solutions of the dimer are light sensitive and were protected from light except during the photolyses. THF was distilled from benzophenone ketyl, tetraglyme (tetraethyleneglycol dimethyl ether, Aldrich) was distilled from CaH_2, and CCl_4 was distilled twice from P_2O_5 and passed through a column of basic alumina. Solvents were degassed by repeated freeze–pump–thaw cycles.

The solvent mixtures and solutions were prepared in a darkened glove-box. All solutions were 20% by volume in CCl_4 (2 M), with various ratios of THF and tetraglyme. (The latter varied from 0 to 80% of the volume of the solution.) Kinematic viscosities of the solution were measured with a calibrated Cannon–Fenske viscometer and are corrected to absolute viscosity. Solutions of **1** were prepared in a darkened glove-box and transferred to 1 cm cuvettes equipped with a magnetic stir bar and an attached freeze–pump–thaw bulb. The samples were degassed for four freeze–pump–thaw cycles and then thermally equilibrated for at least 1 h. The quantum yields in Table 1 represent a minimum of two runs at each viscosity.

Photochemical reactions were carried out with an Oriel 200-W high pressure mercury arc lamp coupled to a monochromator. Light intensity was determined by the power reading in watts on the Merlin apparatus, which was calibrated by actinometry with Aberchrome 540 ($\Phi_{540\ nm} = 0.0484$) [20]. The quantum yields for disappearance of **1** at 540 nm ($I_a = 1.20 \times 10^{-9}$ Einstein s^{-1}) were determined by initial (less than 10%) rates of disappearance of the absorbance at 540 nm. The stirred cells were maintained at constant temperature by using a circulating-water bath to pump chilled water through the cell holder during photolysis. All quantum yields were corrected with a linear correction for non-absorption.

3.2. The apparatus for measuring quantum yields

A schematic diagram of the device and the experimental set-up is shown in Fig. 4. In our system, a 200 W Hg arc lamp serves as the light source, but any type of lamp with contin-

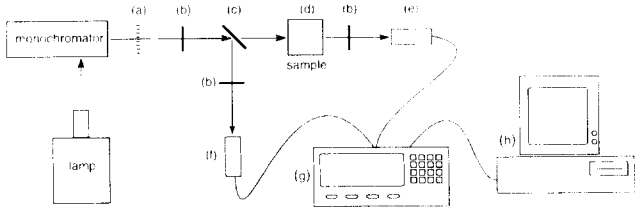

Fig. 4. Schematic diagram of the experimental set-up for the automatic determination of quantum yields (200 W Hg arc lamp; monochromator): a, chopper; b, focusing lens; c, beam splitter; d, water-cooled sample cell holder on magnetic stir plate; e, sample detector head; f, reference detector head; g, Merlin™ control unit; h, computer.

uous output can be used. To eliminate stray radiation, the lamp is enclosed in a box, cooled by a fan. The light beam is passed through a water filter to remove IR wavelengths and then focused on the inlet slit of a monochromator. The intensity and homogeneity of the light beam are maximized visually at this point using the lens-focusing adjustment on the lamp. The beam is then passed through a chopper, which rotates at a frequency of 30.0 Hz to eliminate line noise. The light beam passes through a focusing lens and then a beam splitter. As shown in the diagram, part of the beam is focused with a lens and then sent to the reference detector head of a radiometer. The other beam is the photolysis beam; it passes through the sample cell holder and then a focusing lens before impinging on the signal detector head of the radiometer [21].

Both detector heads are 100 mm^2 silicon photovoltaics (Oriel Corporation model 70111). These photovoltaics can be used in the range 400–1100 nm and are capable of being adjusted to a wide range of light intensities. Data is transmitted from the detector heads to an Oriel Corporation Merlin™ radiometer control unit. This commercial radiometer takes the raw power data from the signal detector head, subtracts the background level, performs calibration corrections and outputs the data in the desired units (e.g. watts) to a personal computer. Calibration corrections are required because the responsivity of the detector head is wavelength dependent. In our system, the detector is calibrated manually using the actinometer Aberchrome™ 540P [20]. (However, for a fee, Oriel will calibrate the detector heads at the time of purchase.) As a matter of sound technique, we always recheck the calibration prior to data collection.

3.3. Using the apparatus

The Merlin™ radiometer collects the intensity of the transmitted light as a function of time and then stores the data on a personal computer (IBM compatible) using the Oriel program RUNES. Normally, the RUNES program is used to control a stepping monochromator but, by adjusting the starting wavelength, the end wavelength, the wavelength interval, and the time between readings, the wavelength base becomes a time base [22]. The resulting file from each photolysis experiment is saved in a .PRN file. The file is imported into QuattroPro for Windows and the data are parsed into two columns and then pasted into a QuattroPro template which is then used to calculate the quantum yield. The template has the following user defined fields: wavelength of irradiation, incident intensity I_0 and extinction coefficient for the species being monitored. I_0 is determined by averaging the light intensity at the sample detector head (with no sample in the holder) immediately before and after the photolysis run. The data are in columns labeled "counts" and "intensity". By using the spreadsheet, these two columns are then converted into "time" and "absorbance" (by using the relation $A = \log(I_0/I_t)$). A plot of absorbance vs. time is displayed, the plot is analyzed by linear regression, and the quantum yield is calculated using the usual expression [23]. Fig. 5

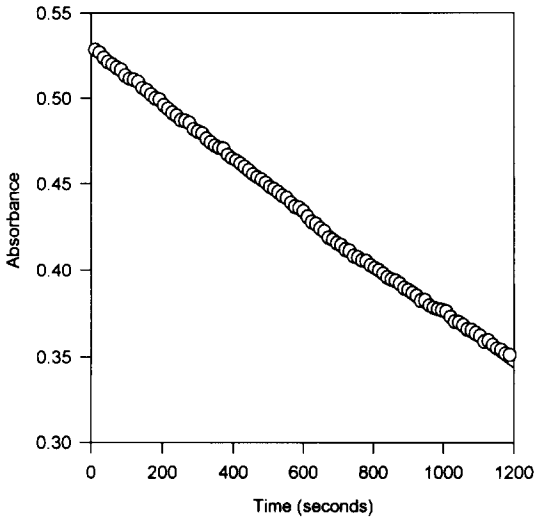

Fig. 5. Plot of absorbance ($\lambda = 540$ nm) vs. time for the photochemical reaction ($\lambda = 540$ nm) of **1** with CCl_4 to form $(CpCH_2CH_2NHCO(CH_2)_3CH_3)Mo(CO)_3Cl$.

shows an example of a plot of absorbance vs. time for the reaction of $(CpCH_2CH_2NHCO(CH_2)_3CH_3)_2Mo_2(CO)_6$ with CCl_4 (2 M in THF; 0.428 cP) to form $(CpCH_2CH_2NHCO(CH_2)_3CH_3)Mo(CO)_3Cl$. (Analysis of the data gives a quantum yield of 0.73 ± 0.02 in this case.)

The data sets collected with the computerized system typically have a minimum of 100 data points with one data point collected every 12 s. However, the system is capable of collecting data every 0.1 s [24] with data set size limited by computer memory. The larger data sets allow for more accurate tracking of the change in transmittance as a function of time. This has its advantages in that power fluctuations in the lamp intensity and other random errors are minimized. The ease of using the system described here needs to be emphasized. Monitoring the reactions and measuring the light intensities are no longer the most difficult parts of measuring quantum yields. Instead, most of the drudgery is now involved in sample preparation. Finally, it is also note worthy that the system described here is easily reconfigured for other experiments.

Acknowledgments

Acknowledgment is made to the National Science Foundation (NSF) for support of this research. In addition, B.E.L. acknowledges the National Physical Science Consortium for a fellowship; A.G.G. was supported by an NSF ROA grant; and G.F.N. was partially supported by a Department of Education GANN fellowship.

References and notes

[1] See for example: (a) A. Rembaum and M. Szwarc, *J. Chem. Phys., 23* (1955) 907; (b) W.A. Pryor and K. Smith, *J. Am. Chem. Soc., 92* (1970) 5403.

[2] (a) H. Kiefer and T. Traylor, *J. Am. Chem. Soc., 89* (1967) 6667; (b) T. Koenig and J.A. Hoobler, *J. Am. Chem. Soc., 93* (1971) 938; (c) T. Koenig and M. Deinzer, *J. Am. Chem. Soc., 90* (1968) 7014.

[3] (a) J. Franck and E. Rabinowitch, *Trans. Faraday Soc., 30* (1934) 120; (b) E. Rabinowitch and W.C. Wood, *Trans. Faraday Soc., 32* (1936) 1381; (c) E. Rabinowitch, *Trans. Faraday Soc., 33* (1937) 1225.

[4] (a) R.M. Noyes, *Z. Electrochem., 69* (1960) 153; (b) R.L. Strong, *J. Am. Chem. Soc., 87* (1965) 3563; (c) S. Kodama, *Bull. Chem. Soc. Jpn., 35* (1962) 658; (d) S. Kodama, *Bull. Chem. Soc. Jpn., 39* (1966) 1009; (e) R.F. Hutton and C. Steel, *J. Am. Chem. Soc., 86* (1969) 745; (f) I. Abram, I.G. Milne, B. Solomon and C. Steel, *J. Am. Chem. Soc., 91* (1969) 1220; (g) Y. Schaafsma, A. Bickel and E.C. Kooyman, *Tetrahedron, 10* (1960) 76.

[5] (a) T. Koenig and H. Fischer, in J. Kochi (ed.), *Free Radicals*, Vol. 1, Wiley, New York, 1973, Chapter 4; (b) T. Koenig, in W.A. Pryor (ed.), *Organic Free Radicals*, in *Am. Chem. Soc., 69* (1978) Chapter 3.

[6] (a) N.J. Turro and B. Krautler, *Acc. Chem. Res., 13* (1980) 369; (b) N.J. Turro, *Proc. Natl. Acad. Sci. USA, 80* (1983) 609.

[7] (a) G. Closs, *J. Am. Chem. Soc., 91* (1969) 4552; (b) R. Kaptein and R. Oosterhoff, *Chem. Phys. Lett., 4* (1969) 195; (c) R. Kaptein and R. Oosterhoff, *Chem. Phys. Lett., 4* (1969) 214; (d) A.R. Lepley and G.L. Closs (eds.), *Chemically Induced Magnetic Polarization*, Wiley, New York, 1973; (e) D. Bethell and M.R. Brinkman, *Adv. Phys. Org. Chem., 10* (1973) 53; (f) R. Kaptein, *Adv. Free Radical Chem., 5* (1975) 319.

[8] T. Koenig, B.P. Hay and R.G. Finke, *Polyhedron, 7* (1988) 1499.

[9] T. Koenig, T. Scott and J.A. Franz, in T. Marks (ed.), *ACS Symp. Ser., 428* (1990) 113–132.

[10] T. Koenig and R.G. Finke, *J. Am. Chem. Soc., 110* (1988) 2657.

[11] (a) For the cage effect see: J.P. Lorand, *Prog. Inorg. Chem., 17* (1972) 207; (b) for diffusion-limited reactions see: S.A. Rice, *Comprehensive Chemical Kinetics*, Vol. 25, Elsevier, Amsterdam, 1985.

[12] Note that the F_c value for a photochemically formed cage pair does not necessarily equal the F_c value for the same caged pair formed by thermolysis or by diffusional collision of two free radicals. In order to differentiate these cases where needed, the photochemical cage efficiency factor is often denoted F_{cp}.

[13] K.J. Covert, E.F. Askew, J. Grunkemeier, T. Koenig and D.R. Tyler, *J. Am. Chem. Soc., 114* (1992) 10446.

[14] Other devices for electronically measuring reaction quantum yields or fluorescence quantum yields have been described previously. However, each is significantly different from the radiometer described herein. For example, the system described by Baumann et al. [15] uses an excitation beam perpendicular to a monitoring beam from a UV–visible spectrophotometer instead of just one beam as used in our system. Furthermore, to our knowledge no system described in the literature uses a computer to control both the acquisition and the analysis of data. Finally, by using a commercial radiometer, our system is easily "constructed" by non-electronics experts. This feature in particular should make the present system exceedingly appealing to photochemists.

[15] H. Baumann, K. Behrmann, H. Jahnke, W. Ortmann and G. Waldmann, *J. Signalaufz. Mater., 5* (1983) 385.

[16] B.E. Lindfors, G.F. Nieckarz and D.T. Tyler, unpublished work, 1995. For more information on polymers that have metal–metal bonds along the backbone, see: (a) S.C. Tenhaeff and D.R. Tyler, *Organometallics, 10* (1991) 473; (b) S.C. Tenhaeff and D.R. Tyler, *Organometallics, 10* (1991) 1116; (c) S.C. Tenhaeff and D.R. Tyler, *Organometallics, 11* (1992) 1466.

[17] M.S. Wrighton and D.S. Ginley, *J. Am. Chem. Soc., 97* (1975) 4246.

[18] T.J. Meyer and J.V. Casper, *Chem. Rev., 85* (1985) 187.

[19] G.F. Nieckarz and D.R. Tyler, *Inorg. Chim. Acta*, accepted.

[20] H.G. Heller and J.R. Langan, *J. Chem. Soc., Perkin Trans. II*, (1981) 341.

[21] A heavy black plastic sheet is used to isolate the light table from any stray light. Currently, the reference detector is not used. However, with an additional circuit board (available from Oriel), the reference data could be used to determine the lamp intensity at all times during the data acquisition.

[22] For example, a starting wavelength of 0.00 nm, an end wavelength of 120.0 nm, a wavelength interval of 1.20 nm and a wait time of 12 s results in 10 s for every wavelength. Therefore the end wavelength is equal to irradiation for 1200 s.

[23] The quantum yield equation is $\Phi = -[(dA/dt)v100]/(I\epsilon\ \%A_{avg})$ where Φ is the quantum yield, dA/dt the slope of the linear regression plot of absorbance vs. time, v the volume irradiated, I the intensity of light, ϵ the molar extinction coefficient at the irradiation wavelength and $\%A_{avg}$ the average percentage absorbance to correct for any non-absorption.

[24] The lower limit of 0.1 s for the wait time is software based. The hardware is capable of instantaneous data acquisition; however, a wait time of zero would make the required conversion to the time base impossible.